УДК 621.039.531:620.178.1

INVESTIGATION OF LONG AND SHORT TERM IRRADIATION HARDENING OF P91 AND P92 FERRITIC/MARTENSITIC STEELS

M.Q. Hiwa[1], M.H. Ari[2]

[1]Department of Physics, College of Science, University of Raparin, Sulaimanyah, Iraq
[2]Department of Physics, Faculty of Science and Health, Koya University, Erbil, Iraq

The aim of the study was to determine the effect of proton irradiation at room temperature on ferritic/martensitic P91 and P92 steels, in particular on their hardness. In addition, SRIM programme was used to identify the proton penetration depth. The study has found that the hardness of the unirradiated P92 steel is higher than that of unirradiated P91 steel, since P92 steel contains tungsten, which produces higher level of solid solution hardening. P91 and P92 steel samples were irradiated using 1.9-MeV protons to the fluence of 1.35×10^{17} ion/cm^2. It was found that Vickers hardness test values increased for both P91 and P92 steels at 0.2 kg loads. For high proton irradiation (long irradiation period) the fluence was 1.101×10^{18} ion/cm^2 (about ten times higher than at the low proton irradiation). With growth of irradiation fluence, the number of displacements per atom (dpa) went up from 0.043 dpa (for low irradiation) to 0.18 dpa (for high irradiation) and the hardness of steels that were under investigation increased. P91 and P92 steel samples after long irradiation were heat treated for one hour at 700 ºC in a vacuum furnace. The study identified that while the chemical composition of P91 and P92 steel were almost identical, irradiated P92 steel requires twice the heat treatment to reduce its hardness to a basic value, as compared with P91 steel samples.

Key words: SRIM, SEM, dpa, P91 steel, P92 steel.

ИССЛЕДОВАНИЕ УПРОЧНЕНИЯ ФЕРРИТНО-МАРТЕНСИТНЫХ СТАЛЕЙ P91 И P92 ПРИ ДЛИТЕЛЬНОМ И КРАТКОВРЕМЕННОМ ОБЛУЧЕНИИ

М.К. Хива[1] и М.Х. Ари[2]

[1]Физическое отделение Научного колледжа Университета Рапарин, Сулеймания, Ирак
[2]Физическое отделение Факультета науки и здравоохранения Университета Коя, Эрбиль, Ирак

Целью данного исследования было определение влияния облучения протонами при комнатной температуре на ферритно-мартенситные стали P91 и P92, в частности, на их твёрдость. Кроме того, для изучения глубины внедрения протонов в стали была использована вычислительная программа SRIM. Обнаружено, что необлучённая сталь P92 твёрже, чем необлучённая сталь P91. Сталь P92 содержит вольфрам, который способствует упрочнению твёрдых растворов. Образцы сталей P91 и P92 были кратковременно облучены протонами энергией 1,9 МэВ до флюенса $1{,}35\cdot10^{17}$ ион/см^2. Под нагрузкой 200 г их твёрдость по Виккерсу увеличилась. Затем аналогичные образцы были подвергнуты приблизительно в 10 раз более длительному облучению до флюенса $1{,}101\cdot10^{18}$ ион/см^2. С увеличением продолжительности облучения увеличилось число смещений на атом с 0,043 до 0,18 млн$^{-1}$ и увеличилась твёрдость образцов. После более длительного облучения образцы исследуемых сталей были подвергнуты термообработке — помещены на один час в вакуумную печь при температуре 700 ºС. Исследование показало, что, хотя химический состав исследованных сталей почти идентичен, термообработка облучённой стали P92 для снижения её твёрдости до исходного уровня требует вдвое большего времени, чем термообработка образцов стали P91.

Ключевые слова: программа SRIM, сканирующий электронный микроскоп, смещение на атом, сталь P91, сталь P92.

DOI: 10.21517/0202-3822-2019-42-2-81-88

INTRODUCTION

The worldwide energy demand has increased during the 21st century. This demand has spurred on international cooperation to identify ways to meet global energy needs, while at the same time, maintain and improve the environment [1]. Over the past 60 years nuclear fission, has emerged to become reliable baseline sources of economical and clean electrical power [2]. Nuclear power can produce a large amount of energy without environmental effect in comparison with fossil fuel sources [3]. In 2011, 435 nuclear reactors operated around the world, producing 370 GWe of electricity, and capacity is likely to increase by another 108 GWe or 108 units, as more reactors are under construction.

To increase the amount of energy provided by nuclear power, a new generation of reactors, Generation IV, has been developed to generate inexpensive, abundant, reliable power in safe and proliferation resistance reactors [4].

Ferritic/martensitic (F/M) steels are used in some applications of Generation IV reactors, namely in pes, pressure vessels, etc, because there is such a high temperature in this type of reactors [5, 6]. In addition, intensive research has been carried out to find a reliable and long-life material for such specific conditions. Nickel and austenitic steels have low thermal expansion, but availability, cost and thermal conductivity issues provide strong reasons to use an alternative material — ferritic steels. Low ferritic steels in subcritical nuclear reactors still serve well as they have enough high oxidation and strength resistance. However, after 1960s, high ferritic

steels with 9—12% Cr, were developed and the basic 9Cr—1Mo steel become the most commonly used structural material, in nuclear power plants [7, 8].

In 1970 P/T91 steels were developed in the USA for nuclear programme by combustion engineering and Oak Ridge National Laboratory, based on the 9Cr—1Mo tube steel. The creep strength of P91/T91 was enhanced by adding small amounts of N, Nb, and V with optimization of the alloy composition. Around 1984, it was discovered that P91 steel could be used in the ASME codes, and in conventional steam plants. In 1988 the P91/T91 steel was used in Kawagoe gas power plants, in Japan with steam parameters 31 MPa/566 ºC [9]. In the mid 1980s, NF616 steels, which comprise tungsten alloyed 9% Cr steel, were produced for the first time, based on the long-term studies of professor Fujita at the University of Tokyo, on 9—12% Cr steels. The basic idea was to create this new steel adding boron and replacing a part of molybdenum with, approximately 1.8% W. This development spread around the globe and was used by boilermakers, and many steels makers in industry [7, 10].

F/M steel have been widely studied by many research groups [11—13]. This paper investigates mechanical properties (hardness) of P91 and P92 steels at high temperature. Moreover, it considers the effect of irradiation on mechanical properties of P91 and P92 steels at room temperature, more specifically on hardness.

EXPERIMENTAL PROCEDURE

Sample preparation. P91 and P92 steel were investigated in this study. The P92 samples came directly from the factory, meaning they had never been in service. In contrast, the P91 samples were from pipes of a conventional nuclear power station, which had been in service for approximately nine years [14].

Sample preparation involved a number of steps, firstly, circle portions of P91 and P92 steels were cut from the pipes using a band saw, and then a hacksaw was used to cut small specimens. The faces of both samples needed to be flat, with one face polished so that precise measurements of the sample hardness could be possible.

At this point, each sample was from 3 to 6 cm long and of 0.4—0.6 cm thick. The polishing process was time consuming. At the beginning the samples required grinding, which was carried out by SiC paper, with a motorized wheel machine. This had to be repeated several times with different grit size papers, reducing in coarseness. First P120 paper and then P240, P800, P1200 and P2500 were used. The surface of samples after these processes was smooth and ready for polishing.

Fig. 1. The appearance of P91 and P92 samples when they are ready to test, after undergoing cutting, grinding and polishing processes

The samples subsequently underwent diamond polishing. A polishing MD-cloths with different diamond (grain sizes 3 and 1 μm) were used, together with the grinding and a magnetic backing. After polishing was complete, a sample was achieved with a brightened face, similar to a mirror, as shown in Fig. 1. This characteristic was essential in order to obtain accurate optical microstructure, scanning electron microscopy (SEM) [15] and hardness testing.

Optical microscopes were used for viewing samples by transmitted light, and one was used to examine specific microstructural characteristics of the tested specimens, and to reveal their more general micro structural properties. The specimens for optical microscopy were prepared as described before, with the addition of etching. The specimen were dipped in an etchant solution such as 2 ml HNO_3 + 98 ml ethanol for about 50 s. After this, the etched sample was put under a metallurgical microscope and software was used to analyze the image at various degrees of magnification. Fig. 2 shows such optical micrgraphs of as received P91 and P92 steels specimens.

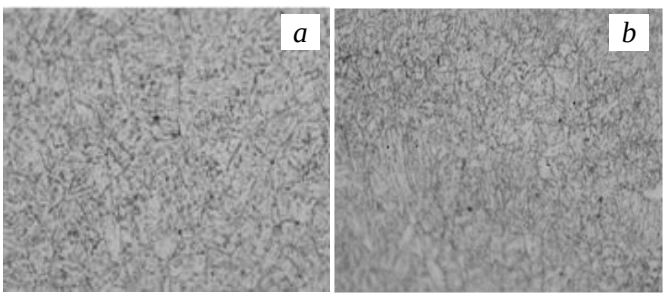

Fig. 2. Optical micrographs of the tempered and normalized (*a*) P91 steel and (*b*) P92 steel

The same P91 and P92 specimens then were put under the scanning electron microscope (SEM), and images were taken at various distances (50, 20, 10

and 5 μm). The SEM testing was used to observe the initial microstructure of specimens, and show grain boundaries of specimens.

Heat treatment of P91 and P92 steels. Following the irradiation of P91 and P92 samples, the Vickers hardness test was carried out, and the effect of irradiation was revealed on the steels. After that, these samples underwent heat treatment for one hour at 700 ºC, and the Vickers hardness tests were repeated to explore whether heat treatment caused a reduction in hardness measures (which had increased as a result of the original irradiation).

Hardness test. Microhardness for P91 and P92 samples was measured using a Vickers hardness machine. The measurements were done at 1 kg and 0.2 kg load. This test analysed unirradiated and irradiated P91 and P92 samples after their heat treatment in order to discover the effect of heat treatment on the hardness values. Fig. 3 shows the Vickers hardness machine used at this study. Hardness values were calculated for both samples to explore the effect of radiation on hardness of these samples. The final reported values were calculated from an average of ten separate readings:

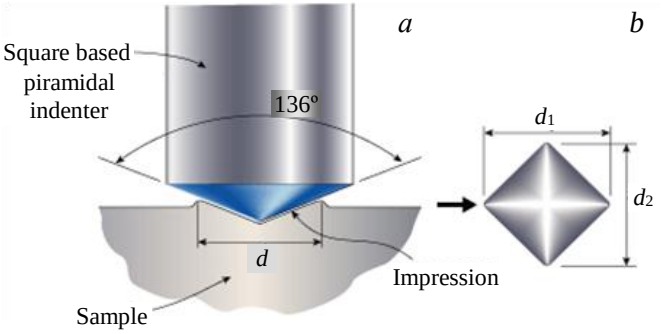

Fig. 3. Vickers indentation (*a*) and measurement of impression diagonals (*b*) [16]

$$d = \sqrt{\frac{1.8544 \cdot F}{H_v}}; \tag{1}$$

$$h = \frac{d}{7.0006}, \tag{2}$$

where H_v is hardness value, d is intender diagonal, F is load and h is indentation depth.

The Eq. 1 was used in this project to find the indenter diagonal, the Eq. 2 also is used in this project to find the depth of indenter at using different loads.

RESULTS AND DISCUSSION

Scanning electron microscopy analysis. The SEM micrographs of the tempered and normalized P91 and P92 steels at different magnification are shown in Figs. 4 and 5 respectively. A tempered martensitic microstructure and austenite grain boundaries can be identified from these figures. The distribution of carbides in the tempered steel is highlighted. The figures reveal inters and intra granular precipitates of various morphologies, such as cylindrical and globular to lenticular. It is evident from Figs. 4 and 5 that the M23C6 carbides are rich in Cr, with small amounts of V, Fe and Mo in the solution.

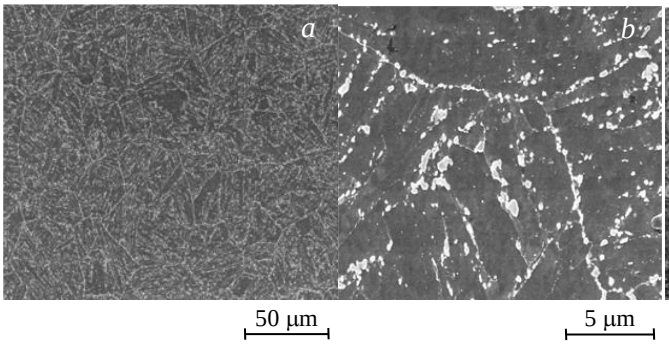

Fig. 4. SEM micrographs of the normalized and tempered P91, (*a*) As received 50 μm of (*b*) As received 5 μm

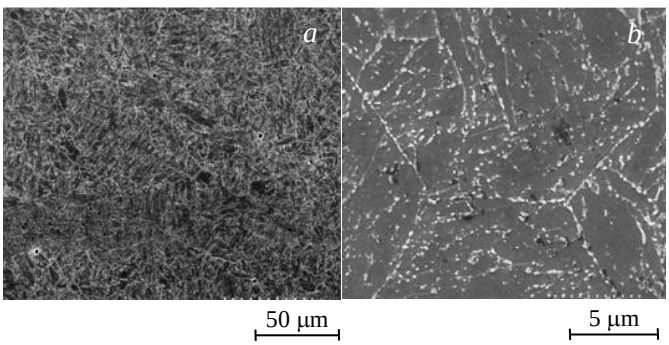

Fig. 5. SEM microstructure of the tempered and normalized P92, (*a*) As received 50 μm (*b*) As received 5 μm

SRIM and TRIM analyseis. The Stopping and Range of Ions in Matter (SRIM), and the Transport of Ions in Matter (TRIM) programmes were both used to calculate the stopping and range of ions from 10 eV to 2 GeV into matter, by using a quantum mechanical treatment of ion-atom collisions [17]. Furthermore, it can be used to gain information about the penetration depth of the ions into the surface of materials [18]. In this paper,

SRIM/TRIM were used to explore the irradiation effect on P91 and P92 steels [19]. Moreover, these programmes were also useful in discovering the penetration depth of proton beams on P91 and P92, by finding the penetration depth of protons. This helped to select a suitable load for the Vickers hardness test.

Firstly, SRIM/TRIM was used to find the penetration depth on 1.9-MeV protons on P91 steel. Fig. 6 shows how penetration depth varies with changing ion energy. It also provides information about the depth of penetration protons into P91 steel. It is found that for 1.9-MeV protons the penetration depth is 17.12 μm, but for 14-MeV proton beam energy, the penetration depth becomes 461.9 μm in P91 steel. It can be seen from Fig. 6 that the penetration depth increases as the proton energy increases. In P92 steel, the penetration depth was 17.15 μm, whereas for 14-MeV protons the depth is 459.28 μm. It is worth noting that at low energies, the penetration depth for P91 is lower than P92. However, at a higher level of energy, beam penetration depth for P92 is lower than P91. This is because P92 steel contains tungsten, which makes it harder.

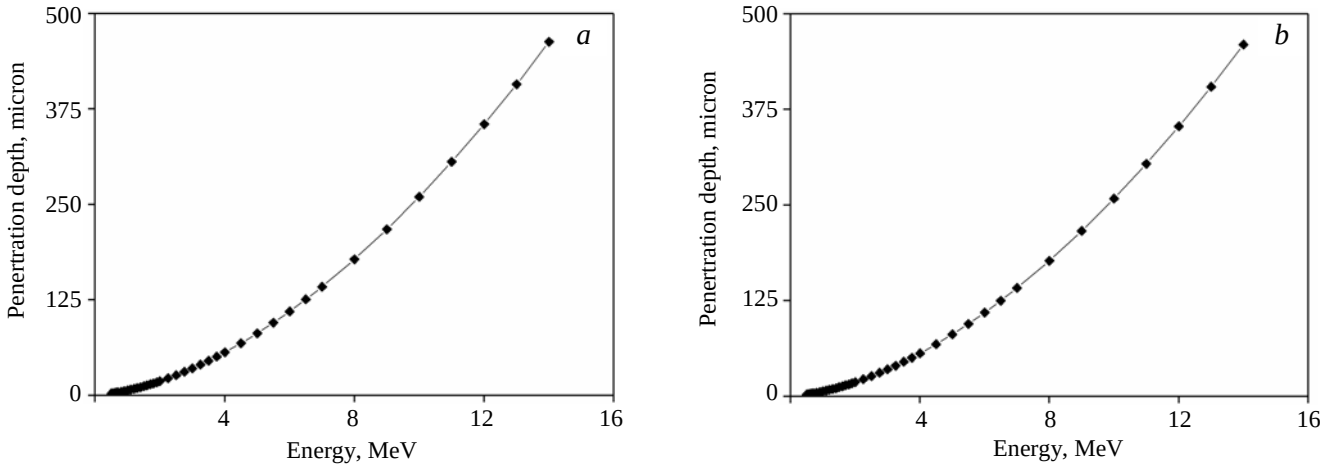

Fig. 6. Penetration depth of proton beam for energy from 0.8 to 14 MeV in P91 (*a*) and P92 steels (*b*)

Another advantage of using SRIM/TRIM is to find the Bragg Peaks (radiation damage area). At almost all radiation damages of P91 and P92 steel atoms, are knocked out of lattices with a large probability that then they will recombine into a lattice.

The number of displacement atoms increases at the Bragg Peaks, because protons lose all their energy on arriving at this depth. The high damage rate occurs at this peak. Therefore, it is important to choice a suitable indenter for a hardness test, which can reach the middle of Bragg peak, in order to measure the exact hardness of the materials.

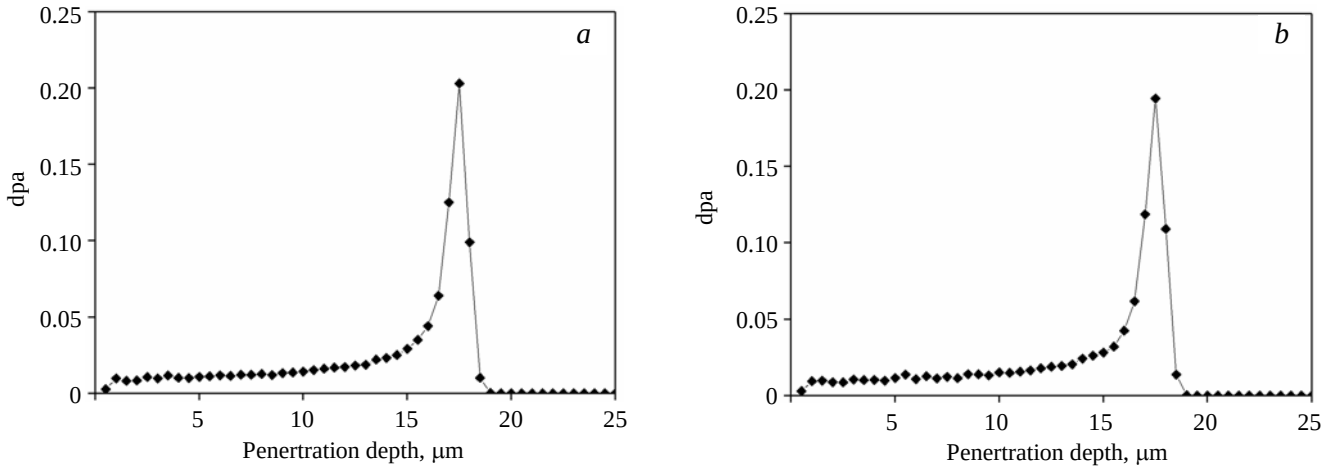

Fig. 7. Bragg peaks in P91 (*a*) and P92 steels (*b*), increase of dpa for 1.9-MeV protons versus proton penetration depth

Long irradiation hardness test. P91 and P92 samples were irradiated with 1.9-MeV protons for 3.5 h. Beam parameters during the proton irradiation on P91 and P92 steels:

Proton energy, MeV . . .	1.9
Irradiated area, cm^2 . . .	0.5
Beam current, μA . . .	7

Proton beam current density, μA/cm^2 . . .	14
Irradiation time, s . . .	12 600
Fluence, proton/cm^2 . . .	1.1×10^{18}

Hardness values were measured for unirradiated and irradiated P91 steel using 1 and 0.2 kg loads. To measure hardness, one row of indentations was made separately for each load, and an average was taken. Vickers hardness test and error were then calculated.

For P91 and P92 steels, Vickers hardness values H_v differ at the 0.2 and 1 kg loads. This difference occurred because of surface plastic and material elastic deformation, which are higher at lower load. These hardness decreased in proportion to an increase in indenter load. This hardness difference for irradiated P91 samples is not significant, and do not greatly affect the results.

By contrast, hardness values for irradiated P91 steel differ considerably for 0.2 and 1 kg loads, as can be seen from Fig. 8. This results from the fact that penetration depth for 1.9-MeV protons is 15.12 μm. Protons lose their energy at this distance. Indeed, after this distance, P91 steel is not irradiated. The probability of interaction increases with decreasing proton energy, which results in number of displacements per atom because dpa increase towards the end of this distance, thus a Bragg peak is created. The indentation depth was identified using Eqs. 1 and 2. The indentation depth with 1 kg loads was 38.07 ± 3 μm as detailed in SRIM/TRIM analysis section. This shows that the indenter went into the unirradiated area, therefore the average hardness values decreased. Whereas the indentation depth with the 0.2 kg load was 16.67 ± 2 μm. This indicates that the indentation depth is not longer than the proton penetration depth, but that the indenter went only to the irradiated depth. The average hardness value is high because the whole indenter depth was irradiated and the indenter reached Bragg peak.

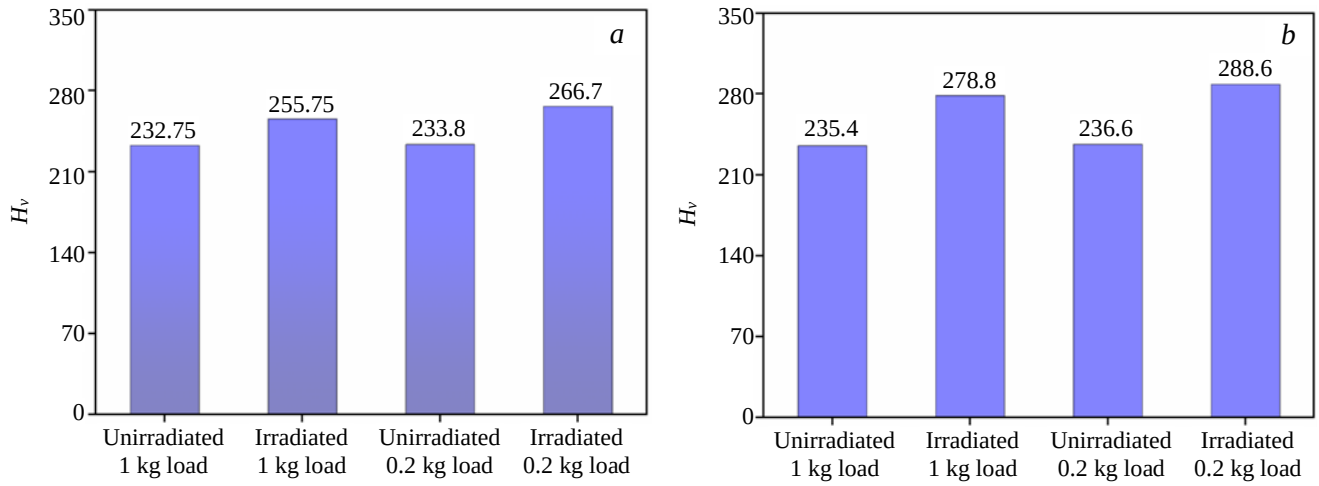

Fig. 8. H_v for unirradiated P91 (*a*) and P92 steels (*b*) using 0.2 kg and 1 kg loads

The Vickers hardness test measured unirradiated P92 samples also with 1 kg and 0.2 kg loads. After the sample underwent proton irradiation at 1.9 MeV, one row of ten indentations was made and then error and mean H_v were calculated.

For unirradiated P92 steel, the hardness test values differed at use of 1 and 0.2 kg loads as well. This was due to plastic deformations on the surface of the material and elastic material deformation. Resistance for both deformations decreased according to an increasing load of the indenter. However, this was not too great, and did not significantly affect the result for unirradiated P92 steel.

On the other hand, it is clear from Fig. 8 that there is a strong difference between hardness test values using 1 and 0.2 kg loads for the irradiated P92 steel. The H_v increased using 0.2 kg load, because it was found in SRIM/TRIM analysis term that a high damage rate occurs at 17.15 μm for P92 steel at 1.9-MeV protons. So, the depth of the indentation was 16,03 ± 2 μm for 0.2 kg load irradiated P92 steel, which is close to Bragg peak, but the depth of the indentation at 1 kg load was 36.5 ± 1 μm, which exceeded irradiated area. It causes to reduce hardness test values using 1 kg load.

Heat treatment of irradiated P91 and P92 steel samples. The irradiated P91 and P92 samples were heat treated for one hour at 700 ºC in a vacuum furnace. Then Vickers hardness test values were measured for unirradiated and irradiated areas of the P91 and P92 steel samples, in order to discover whether the hardness values

maintained the same value, or decreased. A load of only 0.2 kg was used to measure hardness. A row with ten indentations was made for each unirradiated and irradiated area, and then the average was taken.

It can be seen from Table 1 that hardness values for P91 steel decreased rapidly after heat treatment. The hardness test values are approximately the same as before irradiation. This is occurring due to thermally activated recombination and annealing of defects.

Table 1 also demonstrates that hardness test values for heat treated unirradiated P92 steel did not differ too much from similar steel that was not heat treated, because there was no damage. Furthermore, hardness values decreased for heat treated irradiated P92 steel. Nevertheless, it was not decreased to basic hardness value of

T a b l e 1. H_v **for heat treated of unirradiated and irradiated P91 and P92 steels using a 0.2 kg load**

Specimen	H_v
Heat treated unirradiated P91 steel	231.2 ± 3
Heat treated irradiated P91 steel	231.3 ± 2
Heat treated unirradiated P92 steel	234.18 ± 5
Heat treated irradiated P92 steel	248.3 ± 3

unirradiated P92 steels. Therefore the irradiated P92 sample was heat treated for another one hour at 700 °C in the vacuum furnace, to find out if the hardness values more decreases. Table 2 shows that hardness values decreased for P92 steel after the second heat treatment. This study found out that a creep test for P91 and P92 cannot be measured after irradiation. It should be done during the process of irradiation of steels.

T a b l e 2. H_v **after the second heat treatment of P92 steel**

Specimen	H_v
Unirradiated P92	233.9 ± 3
Irradiated P92	237.1 ± 2

Short irradiation. Small portions of P91 and P92 samples were irradiated by 2.8-MeV proton beams for hardness test at the same time and with the same energy. If the whole sample is irradiated, it would remain highly active for a long period, making the experiment very time consuming. The only polished surface was irradiated. The titanium foil window (25 μm) at the end of the beam line also acted as a beam degrader, reducing the beam energy directed at the specimen to around 1.9 MeV. This was used as a beam degrader in the window to reduce the proton beam energy from 2.9 to 1.9 MeV. The proton beam with this energy irradiated P91 and P92 samples.

Proton beam parameters during irradiation on P91 and P92 samples at 1.9 MeV:

Proton energy, MeV . . .	1.9
Irradiated area, cm^2 . . .	0.5
Beam current, μA . . .	6
Beam current density, $\mu A/cm^2$ . . .	12
Irradiation time, s . . .	1800
Fluence, proton/cm^2 . . .	1.35×10^{17}

Unirradiated samples hardness test. Hardness test was re-measured for unirradiated P91 and P92 samples using 1 kg and 0.2 kg loads. Ten measurement indentations were made and an average was generated for each load, allowing a calculation of mean Vickers hardness values. Table 3 lists the hardness test values for these samples in respect of 1 and 0.2 kg loads.

T a b l e 3. H_v **of unirradiated samples, with 1 and 0.2 kg load**

Samples	H_v
P91 steel using 1 kg load	232.8 ± 3
P92 steel using 1 kg load	234.9 ± 2
P91 steel using 0.2 kg load	233.9 ± 5
P92 steel using 0.2 kg load	237.1 ± 3

Table 3 shows that the hardness values for P92 are higher than for P91. This was expected because P92 steel contains tungsten that contributes to steel hardness. Tungsten diffusion slows down recovery and precipitation processes effectively increasing P91 hardness values.

Irradiated samples hardness test. A hardness test was measured for each of the P91 and P92 samples that were irradiated by protons with 1.9-MeV. Ten indentation measurements were made for each P91 and P92 samples and an average taken. The Vickers hardness values were calculated. All hardness test values were obtained with 1 and 0.2 kg loads for each P91 and P92 irradiated samples, and the depth of indenter was calculated for

each load. In addition, the damaged areas were found in each sample using SRIM/TRIM for 1.9 MeV proton beam energy, which helped identify the correct choice of load. This is observable in Table 4.

T a b l e 4. ***H*v for P91 and P92 steel samples, using 1 and 0.2 kg loads**

Samples	H_v
P91 steel using 1 kg load	247.2
P92 steel using 1 kg load	248.3
P91 steel using 0.2 kg load	258.1
P92 steel using 0.2 kg load	259.4

It can be seen from Table 4 and Fig. 9 that the hardness measurement values increase for P91 and P92 steels after being irradiated by protons because radiation causes a raised displacements in atoms within these steels. It can be seen from Tables 3 and 4 that increasing hardness values for irradiated P91 steel is higher than for irradiated P92. This means that irradiation affected P91 steel more strong than P92 steel due to their chemical components.

It is important to note that the hardness values increase with a 0.2 kg load larger than 1 kg load. This is because when a 1 kg indenter was used the depth of indentation was 38.73 for P91 and 38.64 μm for P92 irradiated steels. Whereas the depth of the most damaged area (Bragg peak), for 1.9-MeV proton is 17.12 for P91 and 17.15 μm for P92 steel. These values were identified using SRIM/TRIM computer programs. It is clear that if the indenter goes too

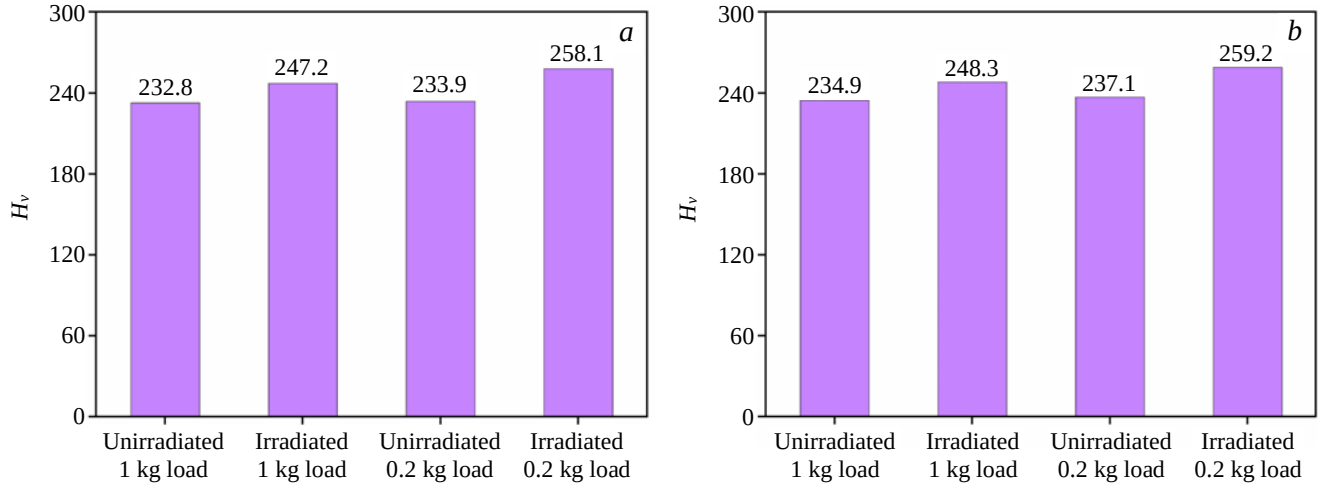

Fig. 9**.** Vickers hardness value for unirradiated and irradiated P91 (*a*) and P92 (*b*) with 1 and 0.2 kg loads

far, the values are not accurate. On the other hand, when the 0.2 kg load indenter was used, the depth of indentation is 16.95 μm for P91 and 16.9 μm for P92 irradiated samples. The indenter goes to the correct area, to the middle of Bragg peak. It is noticeable and significant that these measurements are more precise than others.

CONCLUSION

The effect of ion irradiation, particularly proton irradiation on hardness values of P91 and P92 steel, has been the focus of this investigation. The Vickers hardness test measured for P91 and P92 steel, using 0.2 and 1 kg loads, before and after irradiation. This process identified that the hardness test values for unirradiated P92 steel were higher than for unirradiated P91 steel, because P92 steel contains tungsten, which produces higher level of solid solution hardening. The hardness of both steels increased with increasing proton irradiation. In addition, hardness values increased with a 0.2 kg load compared to use of a 1 kg load. This is due to a variance in penetration depth for protons. The reason for this was found through the SRIM/TRIM programme analysis.

P91 and P92 steel samples after long irradiation were heat treated for one hour at 700 ºC in a vacuum furnace, then the Vickers hardness test were performed on unirradiated and irradiated P91 and P92 samples. It was found that test values were the same as for unirradiated steel hardness. The hardness of irradiated P91 steel sample, after heat treatment decreased and was approximately the same as before irradiation due to the thermally activated recombination and annealing of defects. For P92 steel samples, hardness values after the first heat treatment decreased, not achieving the same hardness values as before irradiation. Therefore, P92 steel samples were heat treated for another one hour at 700 ºC in the vacuum furnace. During the second heat treatment P92 hardness test values decreased. The study identified that while the chemical composition of P91 and P92 steel were almost iden-

tical, irradiated P92 steel requires twice the heat treatment to reduce its hardness value to a basic value compared with P91 steel sample hardness. It was also found out that a creep test for P91 and P92 should be carried out during the irradiation period, due to the thermally activated recombination and annealing of defects.

REFERENCES

1. **Klueh R., Nelson A.** Ferritic/martensitic steels for next-generation reactors. — J. of Nuclear Materials, 2007, vol. 371 (1—3), p. 37.
2. **Adelerhof J., Thoopal M.B., Lee D., Hardy C.** Clean and sustainable fusion energy for the future. — PAM Review: Energy Science & Technology, 2015, vol. 1, p. 20—42.
3. **Javidkia F., Hashemi-Tilehnoee M., Zabihi V.** A comparison between fossil and nuclear power plants pollutions and their environmental effects. — J. of Energy and Power Engineering, 2011, vol. 5 (9).
4. **Committee** UDNERA a Technology Roadmap for Generation IV Nuclear Energy Systems. GIF-002-00. 2002.
5. **Chuvas T.C., Garcia S.P., Pardal J.M., Fonseca Md. P.C.** Influence of heat treatment in residual stresses generated in P91 steel-pipe weld. — Materials Research, 2015, vol. 18 (3), p. 614—621.
6. **Pandey C., Mahapatra M.M., Kumar P., Daniel F., Adhithan B.** Softening mechanism of P91 steel weldments using heat treatments. — Archives of Civil and Mechanical Engineering, 2019, vol. 19 (2), p. 297—310.
7. **Baral J.** Creep Characterization of Boron Added P91 Steel in the Temperature Range 600—650 ºC degree. National Metallurgical Laboratory (NML), 2011.
8. **Anderoglu O., Byun T.S., Toloczko M., Maloy S.A.** Mechanical performance of ferritic martensitic steels for high dose applications in advanced nuclear reactors. — Metallurgical and Materials Transactions, 2013, vol. A 44 (1), p. 70—83.
9. **Abson D.J., Rothwell J.S., Cane B.J.** Advances in welded creep resistant 9—12% Cr steels. — In: 5th Intern. Conf. on Advances in Materials Technology for Fossil Power Plants, 2007.
10. **Zhu P.** Microstructural Evolution in High Chromium Steels. © Pengshu Zhu, 2013.
11. **Shibamoto H., Kimura A., Hasegawa M., Matsui H.** Effects of nickel, phosphorous and sulfur on the post-irradiation annealing behavior of irradiation hardening in Fe—0.2 mass% C—0.3 mass% Cu model alloys. — Materials Transactions, 2019, vol. 60 (1), p. 93—98.
12. **Li Q., Shen Y., Zhu J., Huang X., Shang Z.** Evaluation of irradiation hardening of P92 Steel under Ar ion irradiation. — Metals, 2018, vol. 8 (2), p. 94.
13. **Yang H., Kano S., Mc Grady J., Shen J., Matsukawa Y., Chen D., Murakami K., Abe H.** Surface orientation dependence of irradiation-induced hardening in a polycrystalline zirconium alloy. — Scripta Materialia, 2019, vol. 162, p. 209—213.
14. **Carrizo D.A., Besoky J.I., Luppo M., Danon C., Ramos C.P**. Characterization of an ASTM A335 P91 ferritic-martensitic steel after continuous cooling cycles at moderate rates. — J. of Materials Research and Technology, 2018.
15. **Hardie C.D., Roberts S.G.** Nanoindentation of model Fe—Cr alloys with self-ion irradiation. — J. of Nuclear Materials, 2013, vol. 433 (1—3), p. 174—179.
16. **Testing Nh**. Vickers Hardness Testing. 2018.
17. **Ziegler J.F., Ziegler M.D., Biersack J.P.** SRIM — The stopping and range of ions in matter. — Nuclear Instruments and Methods in Physics Research Section B: Beam Interactions with Materials and Atoms, 2010, vol. 268 (11—12), p. 1818—1823.
18. **Stoller R.E., Toloczko M.B., Was G.S., Certain A.G., Dwaraknath S., Garner FA.** On the use of SRIM for computing radiation damage exposure. — Nuclear Instruments and Methods in Physics Research Section B: Beam Interactions with Materials and Atoms, 2013, vol. 310, p. 75—80.
19. **Shen Y., Zhu J., Huang X.** Ar ion irradiation hardening of high-Cr ferritic/martensitic steels at 700 ºC. — Metals and Materials International, 2016, vol. 22 (2), p. 181—186.

Мухаммед Кадр Хива, магистр наук в области физики и технологии ядерных реакторов, лектор-преподаватель; Научный колледж Университета Рапарин в иракском Курдистане, Ирак

Магдид Хамад Ари, магистр наук в области физики и технологии ядерных реакторов, лектор-преподаватель; Лаборатория ядерных проблем и электроники Факультета наук и здравоохранения Университета Койя в Курдистане, Ирак

Статья поступила в редакцию 4 марта 2019 г.
После доработки 22 марта 2019 г.
Принята к публикации 26 марта 2019 г.
Вопросы атомной науки и техники.
Сер. Термоядерный синтез, 2019, т. 42, вып. 2, с. 81—88.